Recombination dynamics as a key determinant of open circuit voltage in organic bulk heterojunction solar cells: a comparison of four different donor polymers

By *Andrea Maurano, Rick Hamilton, Chris G. Shuttle, Amy M. Ballantyne, Jenny Nelson, Brian O'Regan, Weimin Zhang, Iain McCulloch, Hamed Azimi, Mauro Morana, Christoph J. Brabec,* and *James R. Durrant**

[*]   Prof. J. R. Durrant, Mr. A. Maurano, Dr. R. Hamilton, Dr. C. G. Shuttle, Dr. B. O'Regan, Dr. W. Zhang, Prof. I. McCulloch
Departments of Chemistry, Imperial College London
South Kensington SW7 2AZ (United Kingdom)
E-mail: j.durrant@imperial.ac.uk
        Dr. A. M. Ballantyne, Prof. J. Nelson
Departments of Physics, Imperial College London
South Kensington SW7 2AZ (United Kingdom)
        Dr. H. Azimi, Dr. M. Morana, Prof. C. J. Brabec
Konarka Austria, Altenbergerstrasse 69
A-4040 Linz (Austria)
        Dr. H. Azimi
Christian Doppler Laboratory for Surface Optics
Johannes Kepler University
Linz (Austria)

Solution processed organic solar cells based on blends of semiconducting polymers and soluble fullerene derivatives are showing impressive advances in photovoltaic power conversion efficiency, with recent reports of efficiencies in excess of 6%.[1] One of the key remaining factors limiting the performance of such blend or 'bulk heterojunction' solar cells is that they generally exhibit relatively modest voltage outputs, with the energy corresponding to the open circuit voltage, V_{OC}, typically being less than half the optical gap. This V_{OC} has been shown to be correlated to the energy levels of the donor and acceptor materials of the bulk heterojunction (BHJ).[2] In this paper, we compare the V_{OC} of BHJ fabricated from four

different donor polymers, and show that this voltage depends not only upon the material energetics but also upon the lifetimes of charge carriers within the blend.

Previous studies of the role of material energetics in determining V_{OC} have led to the empirical relation:

$$V_{OC} = (1/e) \ (IP_{donor} - EA_{acceptor}) - 0.3V \qquad (1)$$

where IP_{donor} and $EA_{acceptor}$ are the ionisation potential and electron affinity of the donor and acceptor respectively and the constant $0.3V$ was determined empirically.[2] Other studies have considered alternative factors that can limit V_{OC}, including morphology,[3] shunt resistance,[4] electric field dependent geminate recombination,[5] reverse saturation current,[6] energetic disorder[7] and the presence of interfacial charge transfer states.[8]

We have recently undertaken a study of the role of bimolecular recombination dynamics in limiting the V_{OC} of BHJ devices based upon poly(3-hexylthiophene) (P3HT) : [6,6]-phenyl C_{61} butyric acid methyl ester (PC$_{61}$BM) blend films. In particular, we determined the recombination flux as a function of charge density in the blend film and demonstrated that device open circuit corresponds to the condition when the flux of charge photogeneration (J_{photo}) and bimolecular recombination (J_{rec}) are equal and opposite, i.e.: $J_{photo} = - J_{rec}$. It follows from such analyses that device V_{OC} should be dependent upon the dynamics of recombination, and specifically upon the magnitude of the bimolecular recombination rate coefficient (k_{rec}).[9] Whilst many studies have considered the role of such recombination dynamics in limiting device V_{OC},[5-8] those works have typically not addressed the quantitative relationship between V_{OC} and k_{rec}. In this paper we consider the extent to which this relatively

simple analysis can be extended to calculating correctly differences in open circuit voltage observed between BHJ devices employing different donor polymers.

In the present study we analyze V_{OC} for BHJ solar cells employing four different photoactive layers: P3HT blended with $PC_{61}BM$ (1:1 weight composition) (annealed at 140 ºC), poly(3-hexylselenophene) (P3HS) blended with $PC_{61}BM$ (in 1:1 weight composition) (annealed at 150C), poly[2,6-(4,4-bis-(2-ethylhexyl)-4H-cyclopenta[2,1-b;3,4-b′]dithiophene)-alt-4,7-(2,1,3-benzothiadiazole) (PCPDTBT) blended with [6,6]-phenyl C_{71} butyric acid methyl ester ($PC_{71}BM$) (1:1 weight composition) and poly[(4,40-bis(2-ethylhexyl)dithieno[3,2-b:20,30-d]silole)-2,6-diyl-alt-(4,7-bis(2-thienyl)-2,1,3-benzothiadiazole)-5,50-diyl], here called Si-PCPDTBT, bended with $PC_{71}BM$ (1:1 weight composition) . By employing transient photovoltage, transient photocurrent (TPV/TPC)[9] and charge extraction (CE)[10] techniques, we demonstrate that V_{OC} is dependent not only upon the energy levels of the materials used, but also upon the charge carrier dynamics. In particular we demonstrate a simple relationship between V_{OC} and k_{rec} , which we believe to be a readily applicable and powerful tool to relate device V_{OC} to film interface structure and nanomorphology.

In **Fig.1.a.** we show typical current density – voltage (J-V) curves under simulated AM1.5 illumination for devices made from the four material combinations and the chemical structures and typical IP values reported for the four donor polymers[1].[11-13] The parameters related to these J-V curves, together with the J-V curves in the dark (showing negligible dark leakage losses) are shown in supporting information. It is apparent that the differences in V_{OC} between the devices studied cannot be understood in terms of differences in polymer IP's alone. Both PCPDTBT and Si-PCPDTBT exhibit IP's several hundred meV's greater than P3HT and P3HS, but device voltages only differing by ~100 mV.[11,13] As we show herein,

---

[1] Note the electron affinities of the two acceptors employed here, $PC_{61}BM$ and $PC_{71}BM$, are reported[9] to be very similar. We therefore consider $EA_{acceptor}$ to be the same for all four combinations herein.

this deviation from the trend suggested by the donor IP values can rather be understood by consideration of the bimolecular recombination flux:

$$J_{rec} = -ed\ k_{rec}(n)n^2 \qquad (2)$$

where n is the average electron density, $k_{rec}(n)$ is the charge dependent bimolecular recombination rate coefficient, e is the elementary change and d is the device thickness and we assume for simplicity $n = p$. For annealed P3HT:$PC_{61}BM$ we have shown that n in the photoactive layer of such cells increases as a function of light intensity at open circuit, consistent with the expected splitting of the electron and hole quasi Fermi levels, resulting in a corresponding increase in J_{rec}.[9]

As detailed above, J_{rec} is non-linearly dependent upon n. As such, experimental determination of J_{rec} requires direct measurement of n in the photoactive layer of the device under operating conditions. To achieve this we employ a charge extraction (CE) technique, as detailed previously,[10] to measure n in devices operating at open circuit as a function of bias illumination intensity. The measured n as a function of V_{OC} are shown in **Fig.1.b.** The data for P3HT:$PC_{61}BM$ are in agreement with previous measurements on P3HT:$PC_{61}BM$ devices.[9] In all cases, these data are corrected for electrode capacitances, and for charge recombination losses during extraction.[10] It is apparent that, at matched (one sun) light intensities (marked in red in **Fig.1.b.**), P3HT:$PC_{61}BM$ devices present the highest n. As we show below, this can be attributed to their lower k_{rec}. All the data in **Fig.1.b**. follow the exponential relationship $n = n_0 e^{\gamma V_{oc}}$ where n_0 is the average charge density in the dark and γ is the slope. Values of γ are given in supporting information, and are in all cases less than half the value expected for an ideal bandedge (which would correspond to $\gamma = 1/k_B T$). As previously, this non-ideal behaviour is assigned to the presence of an exponential tail of states

4

extending into the bandgap of photoactive layer, consistent with our previous transient absorption and modelling studies.[9]

Complementing our analyses of charge density, we have employed transient photovoltage (TPV) measurements[9] to determine the charge lifetimes (τ) for the devices under study as a function of n as shown in **Fig.2.a.** Typical raw data are shown in supporting information. In all cases τ shows a power law decrease with n: $\tau = \tau_0 n^{-\lambda}$ where τ_0 is the intercept at $n=0$ and λ is the magnitude of the slope in **Fig.2.a.** Such a power law dependence is consistent with transport limited charge recombination with transport proceeding through an exponential distribution of tail states, although we note the dependence of τ on n is weaker than expected from the tail state function inferred from the bias dependence of n above. This could be explained either by incomplete thermal relaxation of the charge carrier populations or by some recombination occurring directly from tail states; further studies are underway to address this. It is apparent that, at matched n, τ □varies by nearly two orders of magnitude between the polymers, with P3HT:PC$_{61}$BM films exhibiting the slowest decay dynamics and PCPDTBT:PC$_{71}$BM the fastest. The slower decay dynamics for P3HT:PC$_{61}$BM are in agreement with these devices exhibiting the highest n under one sun illumination.

In principle the charge carrier decay dynamics plotted in **Fig.2.a.** may result from either bimolecular recombination or leakage losses due to non-selective device contacts (e.g.: device shorts). Such leakage losses can be readily incorporated in the analysis herein by replacing J_{rec} with a more general loss current $J_{loss}=-edn/[\tau(\lambda+1)]$. However we have previously demonstrated from comparison of transient absorption and photovoltage studies that for P3HT:PC$_{61}$BM devices, bimolecular recombination (i.e.: non-geminate) is the dominant charge loss mechanism (see inset **Fig.2.b.**).[9] We have, moreover, observed similar power law decay dynamics to the TPV dynamics in transient absorption studies of P3HS:PC$_{61}$BM,

PCPDTBT:PC$_{71}$BM and Si-PCPDTBT:PC$_{71}$BM films, suggesting that bimolecular recombination is the dominant loss mechanism under open circuit conditions in all the devices under study. This conclusion is further supported by our observation of power law behaviour of $\tau(n)$ for all the polymers studied herein. Employing this assumption, the $\tau(n)$ data plotted in **Fig.2.a**. can be employed directly to determine k_{rec} as function of n, as shown in **Fig.2.b**.[9] In all cases it is apparent that k_{rec} is a function of n, with a form $k_{rec}(n) = k_0 n^{\lambda-1}$ where k_0 is the intercept at $n=0$ in **Fig.2.b**. It is also apparent that the P3HT:PC$_{61}$BM device exhibits the lowest k_{rec}, consistent with the high degree of phase segregation, and therefore relatively low interfacial surface area reported for such blend films.[14-15] Now we have determined both n and $k_{rec}(n)$ as a function of light intensity at open circuit, we are able employ equation 2. to calculate J_{rec} as a function of device voltage, as illustrated in **Fig.3.a**.

Following our discussion above, **Fig.3.a**. allows us to calculate V$_{OC}$ as the voltage at which, for a given light intensity $J_{SC}=-J_{rec}$ (assuming $J_{photo} \sim J_{SC}$, see discussion below). Mathematically, this corresponds to:

$$V_{OC} = \frac{mk_BT}{e}\ln\left(\frac{J_{SC}}{J_{rec_0}}\right)$$

(3)

where $J_{rec_0} = edk_0n_0^{(\lambda+1)}$ corresponds to the recombination flux extrapolated to V$_{OC} = 0$, and k_0, n_0 and λ have been defined above. The ideality factor m is determined from $mk_BT/e=1/\gamma(\lambda+1)$ where γ is also defined above. Values of these parameters determined for the four polymers and the derivation of this equation are detailed in supporting information. **Fig.3.b**. shows the calculated V$_{OC}$ values determined by equation 3., V_{OC} (calc), versus the measured values V_{OC}(meas) for each polymer at four different light intensities. It is apparent that there is an excellent agreement between these measured and calculated values, with this methodology

calculating the measured V_{OC} to within $\pm$ 15 mV. The agreement between the measured and calculated values of V_{OC}, both as a function of polymer employed and light intensity, strongly supports the key premise of our analysis, namely that open circuit is reached when J_{photo} (or more specifically the flux of generation of dissociated charges) is equal and opposite to J_{rec}.

We note that the determination of $V_{OC}(calc)$ did not require separate measurement of IP_{donor} and $EA_{acceptor}$ as these energy levels are already implicitly included in our measurement of $n(V_{OC})$. Alternatively, equation 3. can be rewritten to make the explicit the dependence of V_{OC} upon these energetics as:

$$V_{OC} = \frac{1}{e}\left(IP_{donor} - EA_{acceptor}\right) + \frac{mk_B T}{e}\ln\left(\frac{J_{SC}}{J_{rec_0}^{BG}}\right) \qquad (4)$$

where $J_{rec_0}^{BG}$ corresponds to the recombination flux determined at $V_{BG} = (IP_{donor}^- EA_{acceptor})/e$. Equation 4 describes three different influences upon V_{OC}. $IP_{donor}^- EA_{acceptor}$ represents the ultimate limit to V_{OC} – corresponding to the condition when the electron and hole Fermi levels reach the acceptor LUMO and donor HOMO energies respectively (we emphasis that the absolute values of IP and EA are only necessary for consideration of the different factors influence V_{OC}, but are not needed for our calculation of $V_{OC}(calc)$). In practice how close these Fermi levels approach the LUMO and HOMO energies depends upon two further factor, the charge photogeneration flux (proportional to J_{SC}) which causes the splitting of the electron and hole quasi-Fermi levels, and the charge recombination flux (proportional to $J_{rec_0}^{BG}$), which at open circuit conditions acts to limit this splitting, as illustrated in the insert to **Fig.3.a.**

We note that Vandewal et al.[8] has recently reported an analysis of device V_{OC} based upon studies of emission from interfacial charge transfer states. We note that such CT states are likely to mediate the bimolecular recombination process focused upon herein. We show in supporting information that both this analysis, and those based upon consideration of the reverse dark current density,[6] are consistent with Eq. 3 above. Also our analysis is consistent with recent studies based upon energy disorder[7] and surface recombination.[16]

Our analysis explicitly demonstrates how V_{OC} depends not only upon the energetics of the blend film (i.e.: $IP_{polymer} - EA_{PCBM}$) but also upon the magnitude of the k_{rec}. For the polymers studied both PCPDTBT and Si-PCPDTBT exhibit ionisation potentials 200-400 meV higher than P3HT, and therefore, in terms of energetics alone might be expected to exhibit higher V_{OC} by 200-400 mV.[11,13] In practice, for the devices studied herein, the V_{OC} increase for these polymers is only ~100 meV. This more modest voltage increase can be understood in terms of the larger k_{rec} determined for these polymers. This results in a larger recombination flux for a given charge density for the two bridged thiophenes based devices. As such the condition $J_{photo} = -J_{rec}$ is reached with the electron and hole Fermi levels further from the LUMO and HOMO energies edges for these polymer:PCBM combinations, resulting in these polymers achieving only a modest net increase in V_{OC} relative to P3HT.

The analysis we propose herein allows us to quantitatively relate V_{OC} directly to k_{rec}. In particular, from the gradients of $J_{rec}(V_{oc})$ in **Fig.3.a.**, it is apparent that a reduction of bimolecular recombination by one order of magnitude will increase V_{OC} of ~ $80mV$. [9] We note that a range of factors can be expected to influence the value of k_{rec} including interface area (and therefore nanomorphology),[3] charge carrier mobilities[17] and interface electronic coupling (including the presence and energetics of interfacial charge transfer states).[6,8] In particular the larger k_{rec} observed for devices employing PCPDTBT, Si- PCPDTBT and P3HS

are consistent with the more modest phase segregation observed in these blend films than in annealed P3HT:PC$_{61}$BM blends. This indicates a direct correlation between V$_{OC}$ and film nanomorphology.[14-15] In addition, differences in the dynamics of charge thermalisation and in and the probability of recombination directly from trap states could influence the different behaviour of the polymers.

A key assumption in our analysis is that J_{photo} does not change between open circuit and short circuit conditions, and can be approximated by J_{SC}. In particular it assumes that any change in macroscopic device electric fields between open circuit and short circuit conditions does not impact significantly upon the efficiency of generation of dissociated charges. The success of the analysis reported herein strongly indicates that this assumption is valid for the devices studied herein. In particular it implies that, at open circuit conditions, the dependence of generation of dissociated charges upon the device electric field is negligible. This conclusion is in agreement with our previous observation, from transient absorption data, that the variation in charge photogeneration between short circuit and open circuit conditions in P3HT:PC$_{61}$BM solar cells is <10%.[9] We note however that this assumption is unlikely to be valid for all organic photovoltaic devices, with for example there being some evidence for electric field dependent charge photogeneration in devices based upon polyfluorene-based polymer:polymer blends.[18] Moreover we note that whilst the assumption $J_{photo} \sim J_{SC}$ is likely to be only approximate, the logarithmic dependence of V$_{OC}$ upon J_{photo} results in this approximation causing only minor errors in our V$_{OC}$ calculation (e.g.: a 30 % error in J_{photo}[11,13,15] would result in only a ~10 mV error in $V_{OC}(calc)$) that validates our analysis for the devices studied herein.

The data report herein was collected for four representative devices. However we have now completed such analyses for other 20 such devices with these materials, including both those

fabricated at Imperial and Konarka. Despite large variations in device performance (including variations not only in *J-V* but also $n(V_{OC})$ and $k_{rec}(n)$), attributable to differences in the details of device fabrication, in all cases we found our analysis of $V_{OC}(calc)$ to be in excellent agreement with $V_{OC}(meas)$. As such, whilst the quantitative data for reported herein should be not taken as typical of all such devices (e.g.: it has been reported that SiPCPDTBT devices can show lower k_{recom} than PCPDTBT devices[13]), our overall analysis appears to have excellent general applicability.

In conclusion, we have proposed a relatively simple approach to analysing the open circuit voltage of polymer:fullerene based organic solar cells, based upon the premise that open circuit is reached when the flux of charge photogeneration (or more specifically the flux of generation of dissociated charges) is equal and opposite to the flux of recombination of these dissociated charges. Empirically our approach is based upon measurement of charge carrier densities and decay dynamics as a function of light intensity, allowing us to take account explicitly of the effects of charge trapping. Employing this approach we are able to calculate correctly the variation in open circuit voltage obtained for four different donor polymers and as a function of light intensity. Our analysis allows us to observe separately the effects of materials energetics (IP_{donor} and $EA_{acceptor}$), charge photogeneration efficiency and recombination kinetics upon device V_{OC}. As such we believe this approach to be an effective tool for achieving the systematic optimisation of the voltage output of organic photovoltaic devices.

Experimental

Materials synthesis and device fabrication methodologies have all been reported previously, including devices fabricated at Imperial and Konarka [11-13]. Generally devices were made by spin-coating blends dissolved in chlorobenzene on top of a layer of PEDOT:PSS onto ITO-

coated glass substrates. Aluminium top electrodes were deposited on the devices that were then annealed. PCPDTBT devices were fabricate with no additive. The thickness for the device tested resulted in a range of 70-90 nm for Si-PCPDTBT:PC$_{71}$BM, 150-170 nm for PCPDTBT:PC$_{71}$BM, P3HT:PC$_{61}$BM and P3HS:PC$_{61}$BM.

The J-V, TPV/TPC and CE were undertaken as been reported previously [9-10], using a nitrogen-dye laser pump pulse with a wavelength of ~620 nm for P3HT:PC$_{61}$BM and P3HS:PC$_{61}$BM devices and ~650nm for PCPDTBT:PC$_{71}$BM and Si-PCPDTBT:PC$_{71}$BM devices. All devices studied showed good agreement with the analysis reported herein, with data shown herein collected with four representative devices.

[1]   M. A. Green, K. Emery, Y. Hishikawa, W. Warta, *Prog. Photovoltaics* **2009**, *17*, 320.

[2]   M. C. Scharber, D. Wuhlbacher, M. Koppe, P. Denk, C. Waldauf, A. J. Heeger, C. L. Brabec, *Advanced Materials* **2006**, *18*, 789.

[3]   J. Liu, Y. J. Shi, Y. Yang, *Advanced Functional Materials* **2001**, *11*, 420.

[4]   H. J. Snaith, N. C. Greenham, R. H. Friend, *Advanced Materials* **2004**, *16*, 1640.

[5]   L. J. A. Koster, V. D. Mihailetchi, R. Ramaker, P. W. M. Blom, *Applied Physics Letters* **2005**, *86*, 3.

[6]   W. J. Potscavage, A. Sharma, B. Kippelen, *Accounts Chem. Res.* **2009**, *42*, 1758.

[7]   G. Garcia-Belmonte, J. Bisquert, *Applied Physics Letters* **2010**, *96*, 113301.

[8]   K. Vandewal, K. Tvingstedt, A. Gadisa, O. Inganas, J. V. Manca, *Nature Materials* **2009**, *8*, 904.

[9]   C. G. Shuttle, B. O'Regan, A. M. Ballantyne, J. Nelson, D. D. C. Bradley, J. R. Durrant, *Physical Review B* **2008**, *78*, 4.

[10]   C. G. Shuttle, A. Maurano, R. Hamilton, B. O'Regan, J. C. de Mello, J. R. Durrant, *Applied Physics Letters* **2008**, *93*, 3.

[11]   D. Muhlbacher, M. Scharber, M. Morana, Z. G. Zhu, D. Waller, R. Gaudiana, C. Brabec, *Advanced Materials* **2006**, *18*, 2884.

[12]   A. M. Ballantyne, L. C. Chen, J. Nelson, D. D. C. Bradley, Y. Astuti, A. Maurano, C. G. Shuttle, J. R. Durrant, M. Heeney, W. Duffy, I. McCulloch, *Advanced Materials* **2007**, *19*, 4544.

[13]   M. C. Scharber, M. Koppe, J. Gao, F. Cordella, M. A. Loi, P. Denk, M. Morana, H. J. Egelhaaf, K. Forberich, G. Dennler, R. Gaudiana, D. Waller, Z. Zhu, X. Shi, C. J. Brabec, *Advanced Materials* **2009**, *21*, 1-4.

[14]   A. M. Ballantyne, T. Ferenczi, M. Campoy-Quiles, T. Clarke, A. Maurano, K. H. Wong, N. Stingelin-Stutzmann, J. S. Kim, J. R. Durrant, I. McCulloch, M. Heeney, J. Nelson, N. W. Duffy, S. Tierney, C. Mueller, P. Smith, *Macromolecules* **2010**, *43*, 1169-1174.

[15]   J. K. Lee, W. L. Ma, C. J. Brabec, J. Yuen, J. S. Moon, J. Y. Kim, K. Lee, G. C. Bazan, A. J. Heeger, *J. Am. Chem. Soc.* **2008**, *130*, 3619.

[16]   T. Kirchartz, B. E. Pieters, K. Taretto, U. Rau, *Physical Review B* **2009**, *80*, 035334.

[17]   A. Pivrikas, G. Juska, R. Osterbacka, M. Westerling, M. Viliunas, K. Arlauskas, H. Stubb, *Physical Review B* **2005**, *71*, 5.

[18]   C. M. Ramsdale, J. A. Barker, A. C. Arias, J. D. MacKenzie, R. H. Friend, N. C. Greenham, *Journal of Applied Physics* **2002**, *92*, 4266.
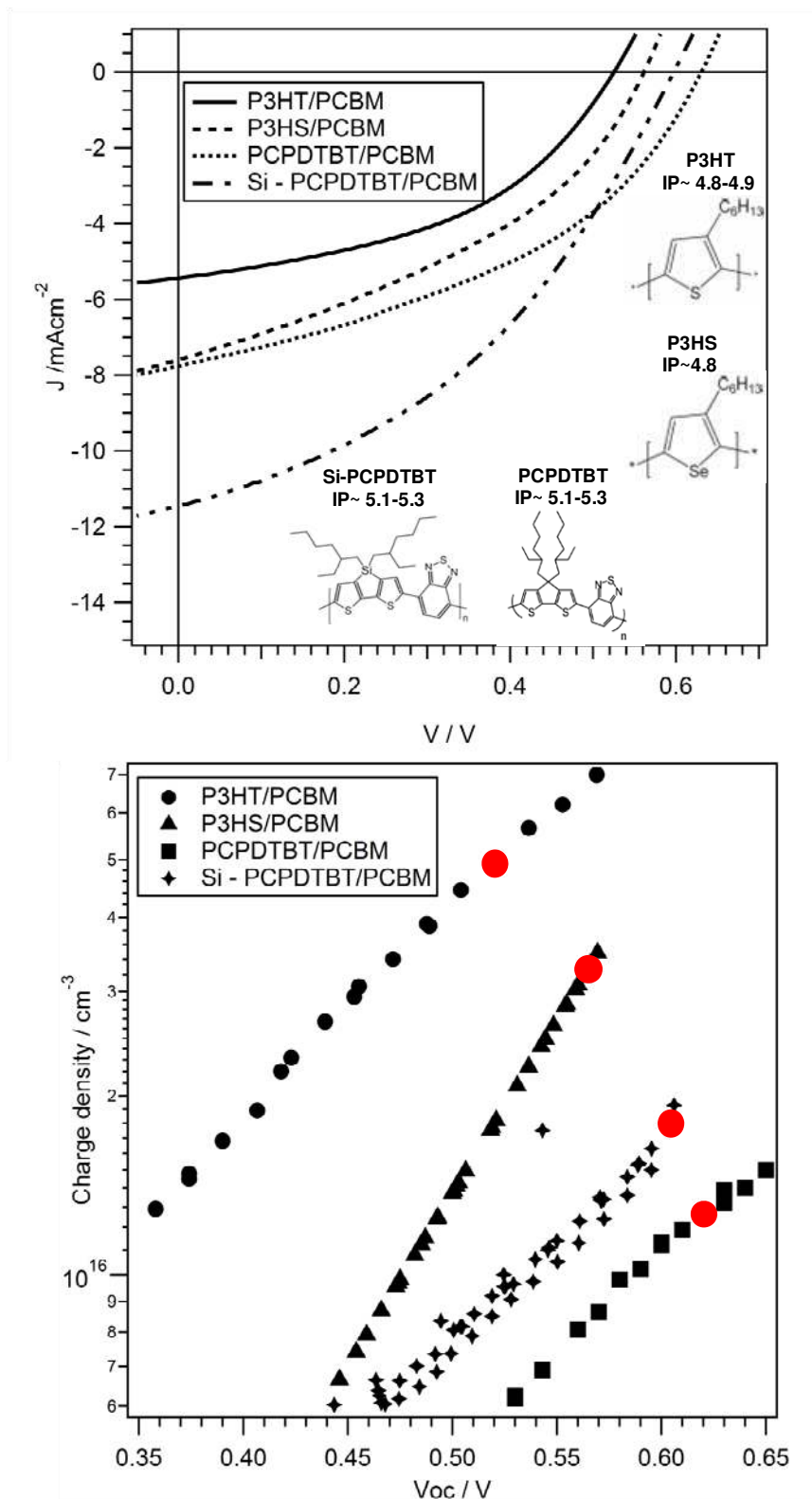
Figure 1. a.) J-Vs under simulated AM1.5 illumination of typical P3HT:$PC_{61}BM$, P3HS:$PC_{61}BM$, PCPDTBT:$PC_{71}BM$ and Si-PCPDTBT:$PC_{71}BM$ BHJ solar cells and polymer structures and typical ionization potentials reported for these polymers.[11-13] b.) Average charge densities measured in these devices operating at open circuit as a function of V_{OC} determined by charge extraction for different bias light intensities. Red dots mark the data points corresponding to one sun light intensity.
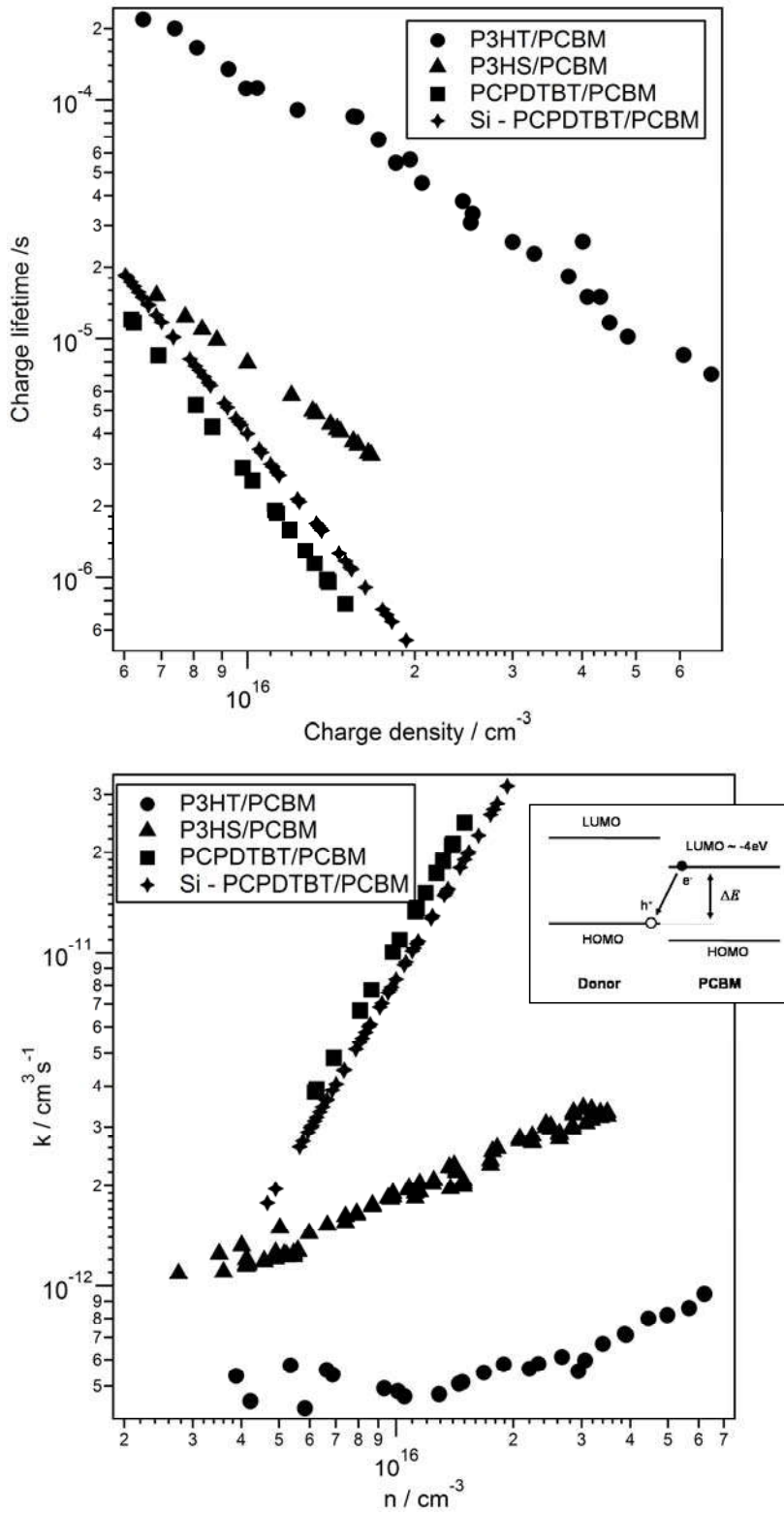
Figure 2. a.) Charge carrier lifetimes as a function of average charge density (*n*) for the four different BHJ devices. b.) The corresponding bimolecular recombination rate constant (*k_{rec}*) as function of *n*. The insert schematic show the bimolecular recombination process.
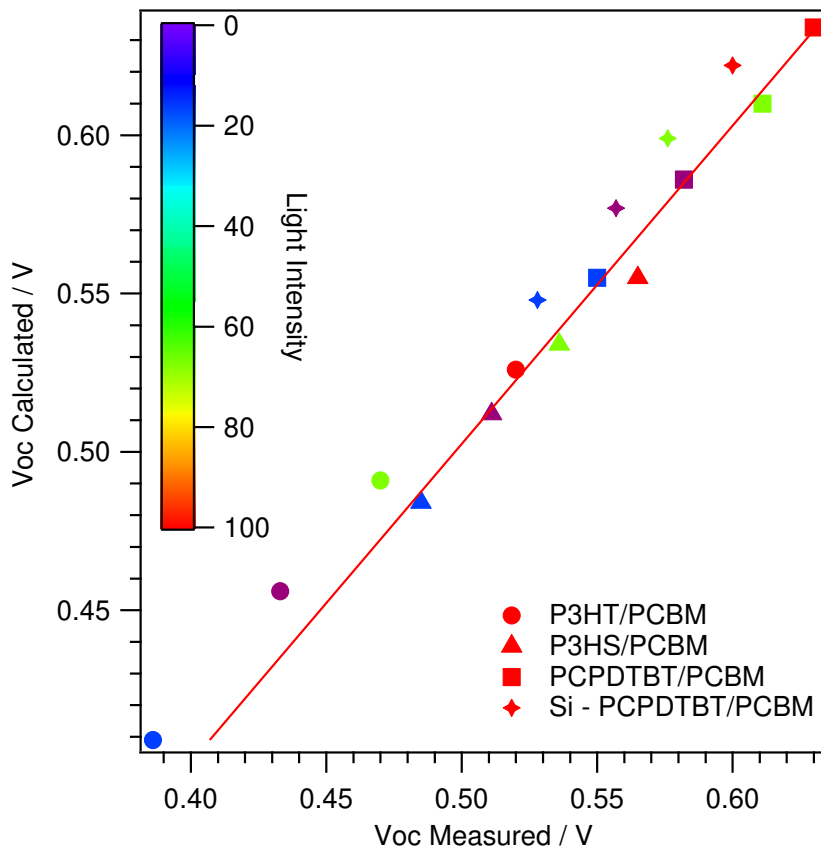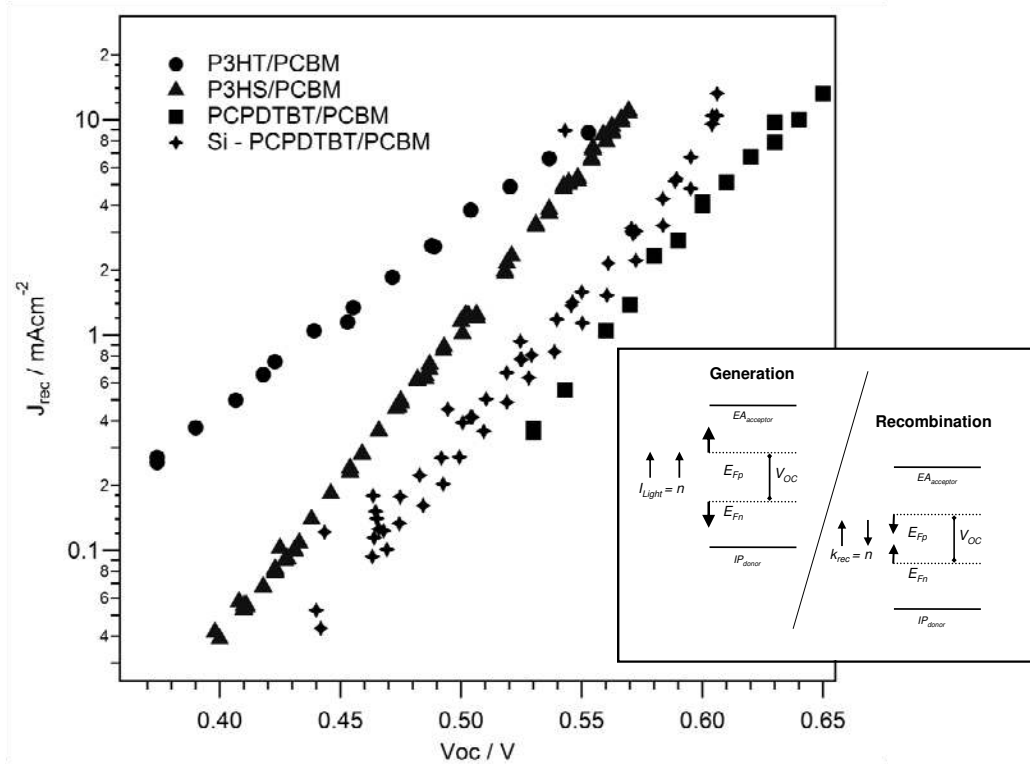
Figure 3. a.) Calculated recombination flux at open circuit (J_{rec}) as a function of V_{OC}. b.) Calculated V_{OC} values determined by equation 3. $V_{OC}(calc)$ versus the measured values $V_{OC}(meas)$ determined from Fig 1.a. for four light intensities.

Supporting information

1. J-Vs parameters under simulated AM1.5 illumination and J-Vs in dark conditions.

We present in **SI Table 1.** the voltage at open circuit (V_{OC}), current density at short circuit (J_{SC}), fill factor (FF) and power conversion efficiency (PCE) for the J-Vs under simulated AM1.5 illumination in Fig.1. Also we show in **SI Fig. 1.** the J-Vs in dark conditions for the devices under study. From the dark currents is evident that the devices under study are not significantly affected by shunt resistance.

Material	Jsc /mAcm^{-2}	Voc / V	FF / %	PCE /%
P3HT	5.40	0.52	~46	~1.28
P3HS	8.00	0.57	~36	~1.62
PCPDTBT	8.00	0.63	~40	~2.02
Si-PCPDTBT	11.50	0.60	~39	~2.71

SI Table 1. Voltage at open circuit (V_{OC}), current density at short circuit (J_{SC}), fill factor (FF) and power conversion efficiency (PCE) for the J-Vs under simulated AM1.5 illumination in Fig.1.
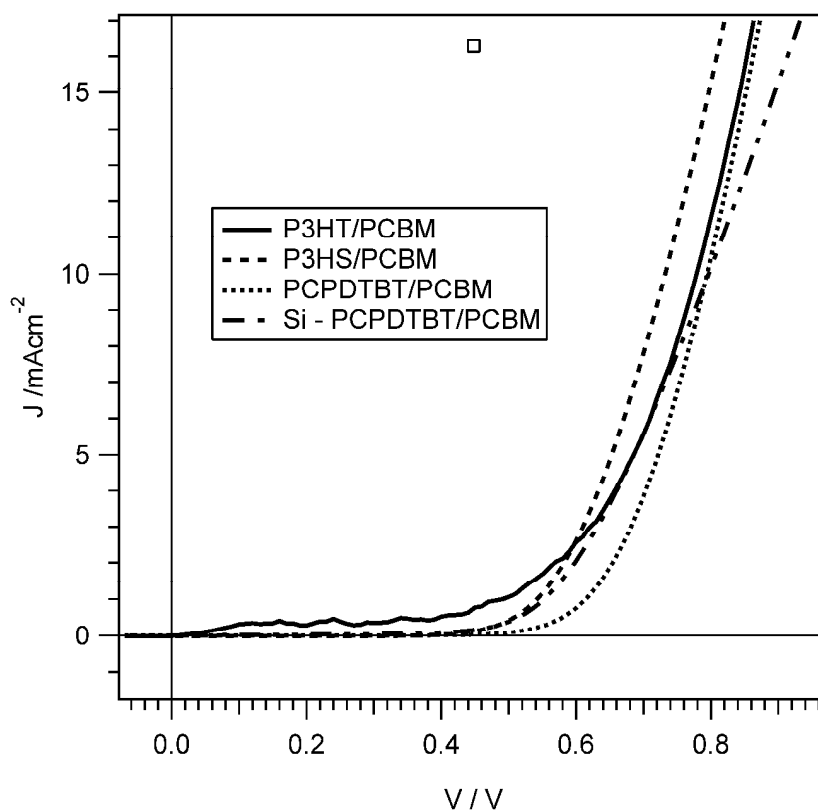
SI Fig.1. J-Vs under dark for the devices under study herein exhibiting negligible device dark shunt losses.

2. Values of γ and λ

We list in **SI Table 2**. the values of the empirical parameters γ and λ obtained with the analysis of TPV transients for the devices under study.

Material	γ /V^{-1}	λ
P3HT	8.09	1.44
P3HS	13.43	1.40
PCPDTBT	7.13	3.10
Si-PCPDTBT	7.68	3.03

SI Table 2. Empirical determined parameters γ and λ for the devices under study

We note that the values in **SI Table 2**. are for four representative devices. However these values may change between devices with the same material, attributable to differences in the details of device fabrication.

3. Raw data acquired with TPV for the devices under study.

We present in **SI Fig. 2**. raw transient data acquired with TPV for the devices under study for a value of the charge density $n\sim10^{16}cm^{-3}$. It is apparent that, at matched n, the lifetime☐vary by nearly two orders of magnitude between P3HT:PC$_{61}$BM and all the other polymers.
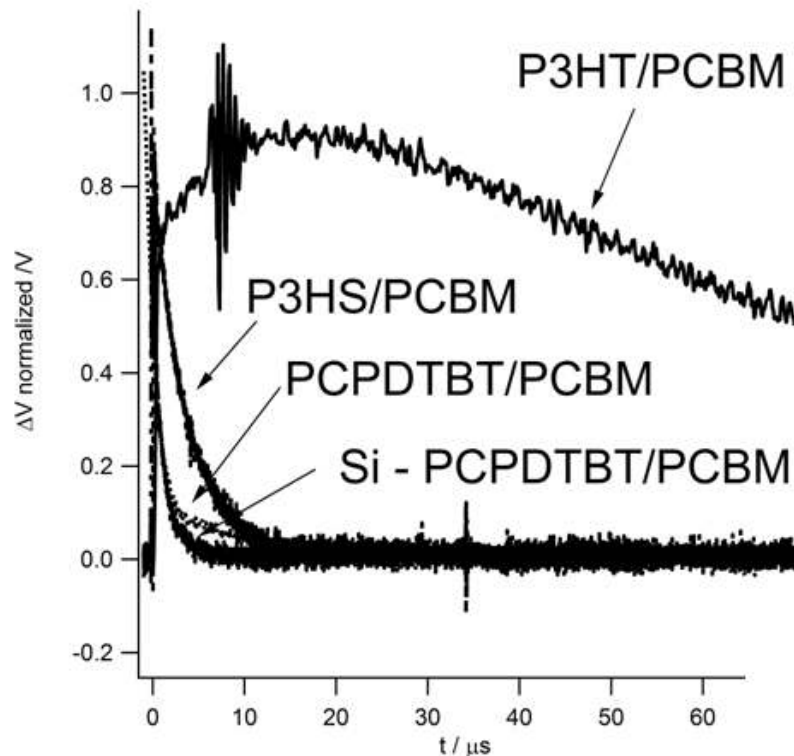
SI Fig.2. Raw transient data for the devices under study.

4. Derivation of equation 3. and equation 4.

The current density under light illumination (J_{light}) can be thought as the sum of the generation current density (J_{photo}) and a loss current density (J_{loss}):

$$J_{light} = J_{photo} + J_{loss} \qquad\qquad \text{SI Eq.1.}$$

We have assumed that $J_{photo} = J_{SC}$, as justified in the paper, and that the electron density is equal to the hole density *(n=p)* in order to express J_{loss} in terms of the charge density n, $J_{loss} = -ed(n/[\tau(\lambda+1)])$ where e is the electronic charge, d the thickness, τ the charge lifetime and λ is an empirical determined parameter as discussed in the paper. We have assigned loss dynamics to bimolecular recombination then: $J_{loss} = J_{rec} = -edk_0 n^{(\lambda+1)}$ where k_0 is the bimolecular recombination rate constant..

Then, at open circuit condition the SI Eq.1. can be rewritten as:

$$0 = J_{SC} - ed\, k_0 n^{(\lambda+1)} \qquad\qquad \text{SI Eq.2.}$$

We have derived the empirical relationship:

$$n = n_0\, e^{\gamma V_{oc}} \qquad\qquad \text{SI Eq.3.}$$

where n_0 is the average charge density in the dark and λ is an empirical determined parameter that can be substituted in SI Eq.2. in order to derive an expression for V_{OC}:

$$V_{OC} = \frac{1}{\gamma(\lambda+1)}\ln\left(\frac{J_{sc}}{edk_0 n_0^{(\lambda+1)}}\right) = \frac{1}{\gamma(\lambda+1)}\ln\left(\frac{J_{sc}}{J_{rec_0}}\right) \qquad \text{SI Eq.4.}$$

where J_{rec_0} is defined as $J_{rec_0} = edk_0 n_0^{(\lambda+1)}$.
SI Eq.3. can also be written as:

$$n = n_0^{BG} e^{\gamma(V_{OC} - V_{BG})} \qquad\qquad \text{SI Eq.5.}$$

where $V^{BG} = (IP-EA)/e$ is the difference between the ionisation potential of the donor (*IP*) and the electronic affinity of the acceptor (*EA*) and n_0^{BG} is the average charge density at V_{BG}. SI Eq.5. can be substituted in SI Eq.2. in order to derive an expression for V_{OC}:

$$V_{OC} = \frac{1}{e}(IP-EA) + \frac{1}{\gamma(\lambda+1)}\ln\left(\frac{J_{SC}}{edk_0 n_0^{BG(\lambda+1)}}\right) = \frac{1}{e}(IP-EA) + \frac{1}{\gamma(\lambda+1)}\ln\left(\frac{J_{SC}}{J_{rec_0}^{BG}}\right) \quad \text{SI Eq.6.}$$

where $J_{rec_0}^{BG}$ is is defined as $J_{rec}^{BG} = edk_0 n_0^{BG(\lambda+1)}$. We used SI Eq.4. to calculated V_{OC} that we have plotted in Fig.3.

Also we note that SI. Eq.4. is consistent with an alternative analysis reported by Vanwal et al.[8] where V_{OC} was calculated using the diode equation:

$$V_{OC} = \frac{kT}{e} \ln\left(\frac{J_{sc}}{J_0} + 1\right) \qquad \text{SI Eq.7.}$$

where k is the Boltzmann constant, T is the temperature and J_0 is the saturation current density. SI Eq.7. is very similar to SI Eq.4. Our formulation is also consistent with the analysis reported by Potscavage et al.[6] where the influence of different interfaces formed in BHJ solar cells on V_{OC} is taken into account. In particular V_{OC} is calculated by:

$$V_{OC} = \frac{nkT}{e} \ln\left(\frac{J_{sc}}{J_0}\right) \qquad \text{SI Eq.8.}$$

where n is a non-ideality factor and J_0 is the saturation current that is assigned to thermal excitation of carriers from the donor to the acceptor materials.